Human Molecular Genetics, 2009, Vol. 18, No. 1 **128–141**
doi:10.1093/hmg/ddn323
Advance Access published on October 10, 2008

BEST1 expression in the retinal pigment epithelium is modulated by OTX family members

Noriko Esumi[1,2,*], Shu Kachi[1,2,†], Laszlo Hackler Jr[1,2], Tomohiro Masuda[1,2], Zhiyong Yang[1,2], Peter A. Campochiaro[1,2,3] and Donald J. Zack[1,2,3,4,5]

[1]The Guerrieri Center for Genetic Engineering and Molecular Ophthalmology at The Wilmer Eye Institute, [2]Department of Ophthalmology, Johns Hopkins University School of Medicine, 832 Maumenee Building, 600 N, Wolfe Street, Baltimore, MD 21287-9289, USA, [3]Department of Neuroscience, The Johns Hopkins University School of Medicine, Baltimore, MD 21287, USA, [4]Department of Molecular Biology and Genetics, The Johns Hopkins University School of Medicine, Baltimore, MD 21287, USA and [5]The McKusick-Nathans Institute of Genetic Medicine, The Johns Hopkins University School of Medicine, Baltimore, MD 21287, USA

Received September 5, 2008; Revised and Accepted October 3, 2008

A number of genes preferentially expressed in the retinal pigment epithelium (RPE) are associated with retinal degenerative disease. One of these, *BEST1*, encodes bestrophin-1, a protein that when mutated causes Best macular dystrophy. As a model for RPE gene regulation, we have been studying the mechanisms that control *BEST1* expression, and recently demonstrated that members of the MITF–TFE family modulate *BEST1* transcription. The human *BEST1* upstream region from −154 to +38 bp is sufficient to direct expression in the RPE, and positive-regulatory elements exist between −154 and −104 bp. Here, we show that the −154 to −104 bp region is necessary for RPE expression in transgenic mice and contains a predicted OTX-binding site (Site 1). Since another non-canonical OTX site (Site 2) is located nearby, we tested the function of these sites using *BEST1* promoter/luciferase constructs by *in vivo* electroporation and found that mutation of both sites reduces promoter activity. Three OTX family proteins – OTX1, OTX2 and CRX – bound to both Sites 1 and 2 *in vitro*, and all of them increased *BEST1* promoter activity. Surprisingly, we found that human and bovine RPE expressed not only *OTX2* but also *CRX*, the *CRX* genomic region in bovine RPE was hypersensitive to DNase I, consistent with active transcription, and that both OTX2 and CRX bound to the *BEST1* proximal promoter *in vivo*. These results demonstrate for the first time *CRX* expression in the RPE, and suggest that OTX2 and CRX may act as positive modulators of the *BEST1* promoter in the RPE.

INTRODUCTION

The retinal pigment epithelium (RPE), a monolayer of cuboidal cells with melanin pigment located between the photoreceptors and choroid of the eye, has many specialized functions that nourish and support retinal photoreceptors (1,2). RPE shares its origin with the neural retina, as both tissues are derived from the neuroepithelium of the forebrain (3,4). Two of the key transcription factors required for RPE specification and development are microphthalmia-associated transcription factor (MITF) and orthodenticle homeobox 2 (OTX2) (3–10). MITF and OTX2 co-localize in the nuclei of the RPE, interact with each other, and can cooperatively activate some genes, such as *QNR71* and tyrosinase (*Tyr*) (11).

MITF is a member of the basic helix-loop-helix leucine zipper (bHLH-ZIP) family of transcription factors and is expressed in several cell lineages, including melanocytes, RPE, osteoclasts and mast cells (6,10,12–14). The MITF-TFE (MiT) subfamily of proteins, which includes

*To whom correspondence should be addressed at. Tel: +1 4105025230; Fax: +1 4105025382; Email: nesumi@jhmi.edu
†Present address: Department of Ophthalmology, Nagoya University School of Medicine, 65 Tsurumacho, Showa-ku, Nagoya, Aichi 4668550, Japan.

MITF, TFE3, TFEB and TFEC, forms homodimers or heterodimers within the subfamily and binds to E-box sequences *in vitro* (6,12). In humans, heterozygous *MITF* mutations result in Waardenburg syndrome type IIA and Tietz syndrome that are characterized by hearing loss and pigmentation defects (15,16). In mice, homozygous *Mitf* mutations ($Mitf^{Mi}/Mitf^{Mi}$) cause pigmentation defects and microphthalmia with thickening of the RPE that forms a multilayered structure resembling the early stage of neural retina (6,8,10,17–19).

OTX2 is a member of the *otd*/*Otx* subfamily of paired-like homeodomain-containing transcription factors (20–23), of which other members in mammals are orthodenticle homeobox 1 (OTX1) and cone-rod homeobox (CRX) (24,25). OTX1 and OTX2 play a pivotal role in anterior head formation and brain development, including multiple aspects of eye development (5,7,22,26,27), whereas the more divergent member CRX, which is orthologous to Otx5 in fish, amphibians and chick (28,29), plays an important role in the development of photoreceptors in the retina and pinealocytes in the pineal gland (30). In humans, heterozygous mutations in *OTX2* were identified in families with ocular malformations, ranging from bilateral anophthalmia to retinal defects resembling Leber congenital amaurosis (LCA) and pigmentary retinopathy (31). Mutations in *CRX* cause autosomal-dominant cone-rod dystrophy (CORD2), LCA and autosomal-dominant retinitis pigmentosa (adRP) (32–35).

In mice, homozygous *Otx2* knockouts ($Otx2^{-/-}$) die early in embryogenesis due to severe defects in gastrulation and a lack of the anterior neuroectoderm fated to become forebrain, midbrain and rostral hindbrain (26,36,37). In the eye, heterozygous *Otx2* knockout mice ($Otx2^{+/-}$) show a wide range of abnormalities that include anophthalmia, microphthalmia, hyperplastic retina and RPE, and a lack of lens, cornea and iris, suggesting multiple roles of OTX2 in eye development (26). In contrast, homozygous *Otx1* knockout mice ($Otx1^{-/-}$) show spontaneous epileptic seizures with abnormalities affecting multiple brain areas, and in the eye reduction of the iris and the absence of the ciliary process are observed (38). In homozygous *Crx* knockout mice ($Crx^{-/-}$) photoreceptor cells are present, but they do not develop normally. The photoreceptors do not elaborate outer segments, the retinas lack rod and cone functional activity as measured by electroretinogram, and the animals show defects in circadian entrainment (30).

Analyses of mice deficient in both *Otx1* and *Otx2* have been helpful in defining the roles of OTX factors in eye development, particularly the development of the RPE (7). All embryos with an $Otx1^{-/-}$; $Otx2^{+/-}$ genotype showed abnormalities in the folding of the optic vesicle into an optic cup, a lack of RPE specification associated with a complete loss of RPE markers, and expansion of the prospective neural retina and optic stalk-like territories. Later in development, the presumptive RPE region of these mice developed into the mature neural retina-like structure. Similar, but less severe phenotypes were observed in 30% of $Otx1^{+/-}$; $Otx2^{+/-}$ mouse embryos, suggesting that *Otx* genes are required in a dose-dependent manner for eye development (7). Supporting such dose-dependent effects of OTX factors, studies of mouse models carrying *Otx1* replaced with human *OTX2* cDNA and vice versa indicated a remarkable functional equivalence of OTX1 and OTX2 proteins (20,39,40). Among the several OTX2 direct targets in the RPE that have been identified so far, all are pigment-related genes, such as *QNR71*, *Tyr*, tyrosinase-related protein 1 (*TYRP1*) and dopachrome tautomerase (*DCT*) (11,41).

Given the essential role of the RPE in supporting and maintaining photoreceptor health and function, and the importance of RPE-specific genes, it seems important to elucidate the mechanisms regulating RPE-specific gene expression. To complement studies such as those described above, we have been analysing the 5′-upstream region of *BEST1* (formerly *VMD2*), a gene that is highly and preferentially expressed in the RPE, as a model system for RPE gene expression (42,43). In addition to the RPE, *BEST1* is expressed in the testis, brain (44), in airway epithelial cells (45) and in melanocytes of the skin [microarray database at the National Center for Biotechnology Information (NCBI)]. *BEST1* encodes bestrophin-1 (also known as bestrophin), a multispan transmembrane protein that seems to function as an oligomeric Ca^{2+}-activated chloride channel implicated in transepithelial fluid transport (44,46–50). Although it has been suggested that bestrophin-1 is a chloride channel and responsible for the light peak in the electrooculogram, it was also proposed that bestrophin-1 is not a chloride channel but rather a regulator of a voltage-dependent Ca^{2+} channel that is required to generate the light peak in the electrooculogram (51,52), leaving its precise physiological function unresolved. Recently, human bestrophin-1 was shown to modulate voltage-gated Ca^{2+} channel $Ca_V1.3$ by interacting with the $Ca_V\beta$ subunit through the C-terminus, supporting that bestrophin-1 is a multifunctional protein acting as both a chloride channel and a Ca^{2+} channel regulator (53). Mutation of *BEST1* causes Best disease [vitelliform macular dystrophy (VMD)], an autosomal-dominant juvenile-onset macular degeneration with characteristic abnormal electrooculogram (44,46), as well as a fraction of adult-onset vitelliform macular dystrophy (AVMD) (49,54,55). Mutations in *BEST1* were also identified in families with nanophthalmos associated with autosomal-dominant vitreoretinochoroidopathy (ADVIRC), suggesting a role for *BEST1* in ocular development (56). Recently, another type of human retinopathy, autosomal-recessive bestrophinopathy (ARB), has been proposed as the null phenotype of bestrophin-1 due to biallelic mutation in *BEST1* (57). ARB patients showed a diffuse irregularity of the reflex from the RPE and an accumulation of fluid within and/or beneath the neural retina in the macular region, without the vitelliform lesions characteristic of Best disease (57).

In our *BEST1* promoter analyses using transgenic mice and cell transfection assays with small-interfering RNAs (siRNAs), we recently demonstrated that the human *BEST1* −154 to +38 bp region is sufficient to direct RPE-specific expression in the eye, and that members of the MITF–TFE family play a major role in regulating the *BEST1* proximal promoter (42). Using *in vivo* electroporation, we also showed that the −154 to −104 bp region contains positive-regulatory elements contributing to a 10-fold difference in *BEST1* promoter activity in mouse RPE, and demonstrated that a canonical OTX factor-binding site is located within this region (43,58). Since we defined *BEST1* as a target of

MITF regulation, these findings raised an interesting possibility that *BEST1* may also be under the control of OTX2, and thereby may present the first example of a non-pigment-related gene that is regulated by both MITF and OTX2. In this paper, we provide evidence that this is indeed the case. We also show that the 'retinal' transcription factor CRX is expressed in the RPE as well as the retina, and suggest that both OTX2 and CRX may act as positive modulators of the *BEST1* promoter in RPE cells.

RESULTS

BEST1 −154 to −104 bp region contains regulatory elements necessary for retinal pigment epithelium expression in transgenic mice

Using transgenic mice, we previously defined the *BEST1* upstream region from −154 to +38 bp as being sufficient to direct RPE-specific expression in the eye (42). To more finely define the minimal regulatory region necessary for RPE expression *in vivo*, we generated transgenic mice with a *BEST1* promoter/*lacZ* construct containing sequence from −104 to +38 bp. Five transgenic founders were obtained, and all were successfully established as independent lines. Analysis of multiple animals from each line by X-gal staining of both RPE/choroid flat-mounts and eye sections, even with staining for up to 72 h, failed to detect positive *lacZ* expression in the RPE as well as other parts of the eye in any of the lines (data not shown). This new result, which indicates that the *BEST1* upstream region from −154 to −104 bp contains positive-regulatory elements necessary to drive expression in the RPE, is consistent with our *in vivo* electroporation data demonstrating that DNA elements in the −154 to −104 bp region can enhance promoter activity by approximately 10-fold (58).

Proximal OTX-binding sites contribute to *BEST1* promoter activity *in vivo*

To define the positive-regulatory elements within the −154 to −104 bp region, additional *BEST1* promoter/luciferase reporter constructs were tested by *in vivo* electroporation of murine RPE (58,59). Deletion of the region between −154 and −137 bp resulted in a 55% decrease in promoter activity (Fig. 1A). Further deletion of the region between −136 and −121 bp resulted in another 21% decrease in activity, and deletion of −120 to −105 bp caused an additional 15% decrease, thus indicating that the regulatory activity in the −154 to −104 bp region is diffusely distributed rather than being localized to a single DNA element.

Based on the presence of a canonical OTX family factor-binding site (AGATTA, Site 1) at −127 to −122 bp and a nearby non-canonical OTX site (GGCTTA, Site 2) at −81 to −76 bp, we experimentally evaluated the potential activity of these sites. Reporter constructs containing mutation in Site 1 (AGATTA to AG*CGGC*, designated ma), Site 2 (GGCTTA to GGC*GGC*, mb) or both (mamb) were generated in the context of the −154 to +38 bp fragment. In D407 human RPE cells that express *BEST1* at low to moderate levels, ma did not show any change in promoter activity, and a reduction in promoter activity by mb was not statistically significant ($P = 0.056$); however, mamb modestly but significantly decreased luciferase activity by 29% ($P = 0.013$) (Fig. 1B). In SK-MEL-5 human melanoma cells that express *BEST1* at high levels, ma again did not affect promoter activity, but mb and mamb significantly decreased promoter activity by 43% ($P = 0.041$) and 46% ($P = 0.026$), respectively (Fig. 1C). In mouse RPE *in vivo*, a 20% decrease in promoter activity by ma was not statistically significant ($P = 0.19$), but mb and mamb reduced luciferase activity significantly by 44% ($P = 0.01$) and 56% ($P = 0.0005$), respectively (Fig. 1D). These differences are most likely due to differential expression of transcription factors and/or their interacting proteins in RPE *in vivo* compared with cell lines. We suggest that the *in vivo* electroporation results, which indicate that the non-canonical OTX Site 2 is the more functionally important of the two, are likely to most closely reflect the *in vivo* situation.

OTX family proteins bind to the *BEST1* proximal promoter *in vitro*

To further explore the possible role of OTX family members in regulating *BEST1* expression in the RPE, we tested the ability of CRX, OTX1 and OTX2 to bind to Sites 1 and 2 *in vitro*. CRX, OTX1 and two isoforms of OTX2 (OTX2-s, short-form, 289 amino acids; OTX2-l, long-form, 297 amino acids) were generated by *in vitro* transcription and translation. Electrophoretic mobility shift assays (EMSAs) were performed with these proteins and four annealed oligonucleotide probes, Probe Site 1 corresponding to −135 to −112 bp, Probe Site 2 corresponding to −91 to −68 bp and Probes ma and mb containing mutations as defined above. Both Site 1 and Site 2 probes yielded shifted bands with all OTX family proteins tested, with slightly stronger binding seen with OTX2; the mutated probes did not show detectable shifts (Fig. 2A). These results indicate that all three OTX family factors can bind to both Sites 1 and 2 *in vitro*, with slightly stronger binding observed with the canonical OTX site (Site 1).

We performed oligomer competition experiments using ^{32}P-labeled Site 1 and Site 2 probes with unlabeled 'competitor' annealed oligonucleotides corresponding to Probes Site 1, ma, Site 2 and mb to assess binding specificity. A similar degree of competition for both labeled probes was observed with the competitors of Sites 1 and 2 (Fig. 2B). Demonstrating sequence specificity, mutated competitor, either ma or mb, did not significantly compete with either probe.

OTX family factors modulate *BEST1* promoter activity through proximal binding sites

Next, we examined functional activities of OTX family factors on the *BEST1* promoter by co-transfection assays using *BEST1* promoter/luciferase constructs and expression vectors for OTX factors in D407 cells. All three OTX family factors including the short and long forms of OTX2 transactivated the *BEST1* −154 to +38 bp promoter in a similar dose-dependent manner (Fig. 3A). To examine whether this transactivation was mediated by the two OTX-binding sites, co-transfection assays were performed in D407 cells using constructs that incorporated the ma and mb mutations in Sites 1 and 2,

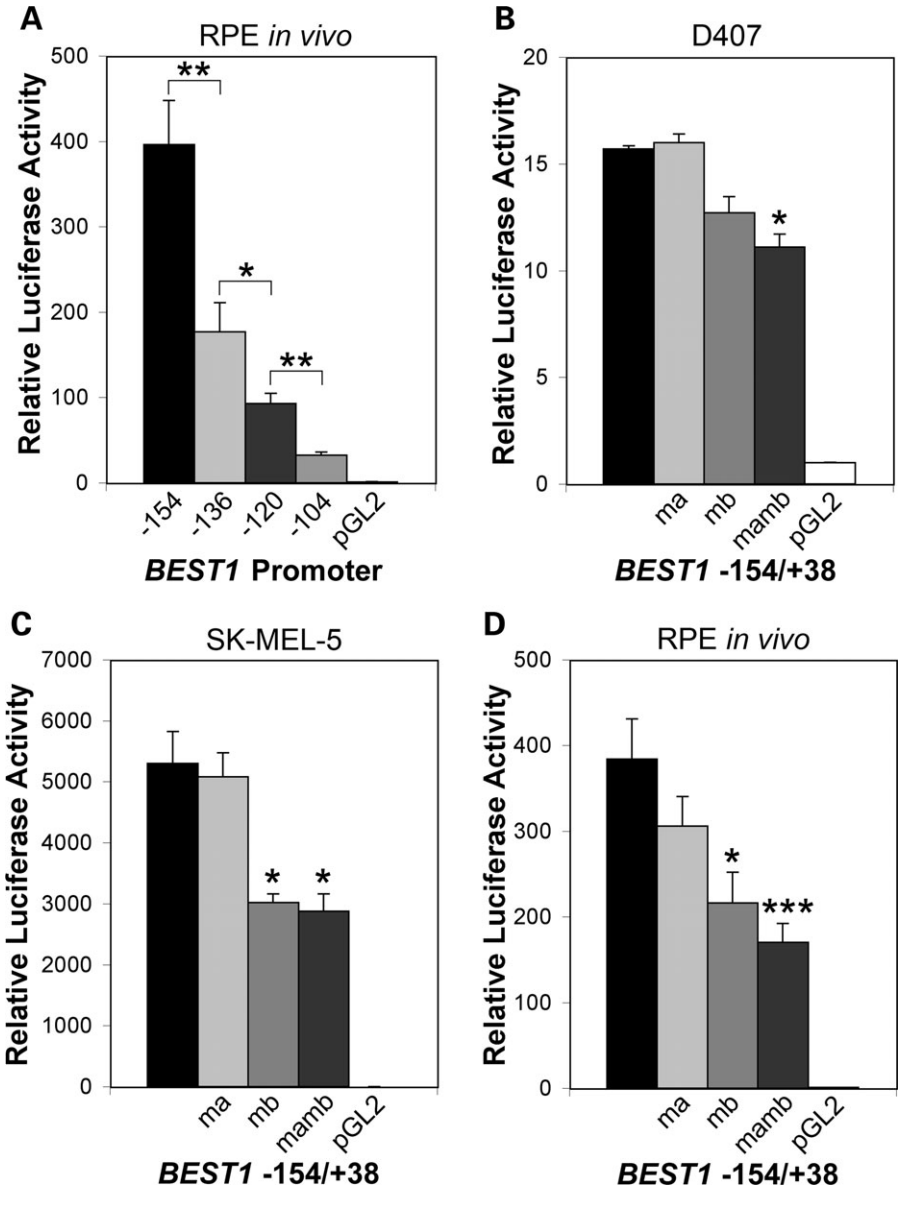

Figure 1. Proximal OTX-binding sites contribute to *BEST1* promoter activity *in vivo*. (**A**) Promoter activity of *BEST1* deletion constructs in mouse retinal pigment epithelium (RPE) *in vivo*. Luciferase constructs containing the *BEST1* −154 to +38 bp, −136 to +38 bp, −120 to +38 bp and −104 to +38 bp fragments or empty pGL2-Basic vector, together with control pRL-CMV for normalization, were introduced into mouse RPE cells by subretinal injection followed by *in vivo* electroporation. Three days later, cell lysates were prepared from the posterior portion of the eyes, and luciferase activities were measured. Firefly luciferase activities were normalized by *Renilla* luciferase activities, and relative luciferase activities (fold increase) were calculated as the ratio of the normalized luciferase activity with constructs containing *BEST1* promoter fragments to that with empty pGL2-Basic vector. After removing unsuccessful subretinal injection and *in vivo* electroporation, the number of valid samples for each construct were between 8 and 19. The values represent the means and SEM (bar). Statistical significance is shown by $^{*}P < 0.05$, $^{**}P < 0.01$ and $^{***}P < 0.001$ throughout Figure 1. (**B**) Effect of OTX site mutation on *BEST1* promoter activity in D407. Luciferase constructs containing wild-type sequence as well as mutation of Site 1 (ma), Site 2 (mb) and both (mamb) in the context of the *BEST1* −154 to +38 bp region were transfected into D407 cells together with control pRL-CMV for normalization. Relative luciferase activities (fold increase) were calculated as described in (A). Transfection experiments were performed three times independently in duplicate each time. The values represent the means and SEM (bar). Statistical significance was examined for each mutated construct compared with the wild-type construct. (**C**) Effect of OTX site mutation in SK-MEL-5. Experiments were performed and results are presented in the same manner as described in (B), except that SK-MEL-5 cells were used as host for transfection. (**D**) Effect of OTX site mutation in mouse RPE *in vivo*. Experimental design was the same as in (B) and (C), except that *in vivo* electroporation was performed to transduce plasmids into native mouse RPE. After removing unsuccessful subretinal injection and *in vivo* electroporation, the number of valid samples for each construct were between 7 and 18.

respectively. Mutation of OTX-binding sites modestly but significantly decreased the transactivation by OTX2-s, with ma, mb and mamb resulting in 21, 36 and 44% reduction, respectively (Fig. 3B). Transactivation by CRX was decreased in a similar manner to that by OTX2-s, resulting in a 31, 45 and 53% reduction by ma, mb and mamb, respectively (Fig. 3C). Of potential significance, the pattern and degree of reduction by the mutated constructs were strikingly similar to the

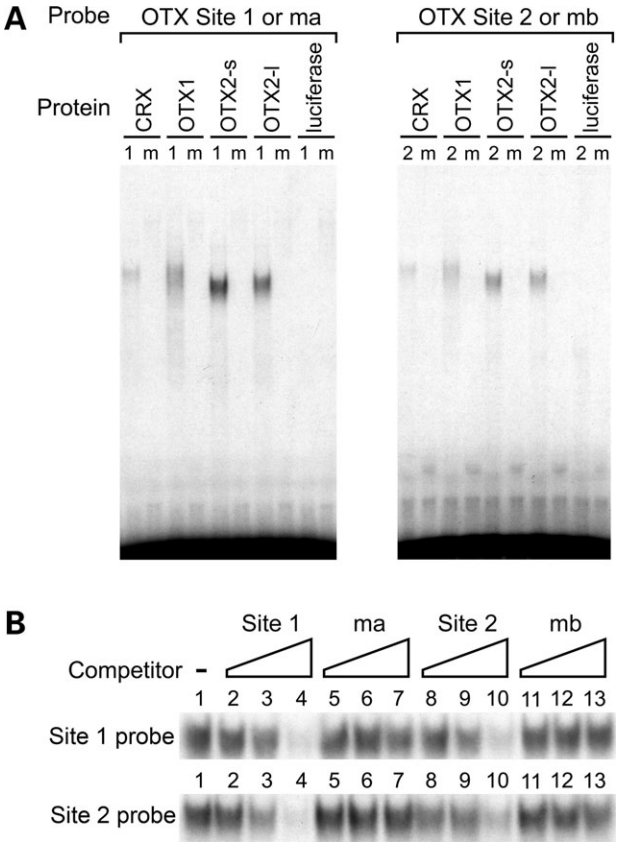

Figure 2. OTX family proteins bind to the *BEST1* proximal promoter *in vitro*. (**A**) Electrophoretic mobility shift assay (EMSA) with OTX family proteins. (Left panel) EMSA was performed with *in vitro* transcribed and translated CRX, OTX1, OTX2-s, OTX2-l and control luciferase proteins and probes containing OTX Site 1, wild-type (lanes labeled '1') and with ma mutation (labeled 'm'). Radiolabeled oligonucleotide probes were incubated with 3 μl of *in vitro* transcribed and translated proteins in the presence of 1 μg poly (dI–dC). The film was exposed overnight without an intensifying screen. Shifted bands were observed with all OTX family proteins and the wild-type probe, but abolished when the probe was mutated. (Right panel) EMSA was performed in the same manner as in left panel, except that probes used were oligonucleotides containing OTX Site 2, wild-type (labeled '2') and with mb mutation (labeled 'm'). Shifted bands were observed with the wild-type probe and all OTX family proteins, but not with the mutated probe. (**B**) Cold oligomer competition. ^{32}P-labeled Site 1 and 2 probes were mixed with 0- (lane 1), 10- (lanes 2, 5, 8 and 11), 100- (lanes 3, 6, 9 and 12) and 1000-fold (lanes 4, 7, 10 and 13) molar excess of unlabeled competitors, and then added to binding solution containing 1 μl of OTX2-s protein and 1 μg poly (dI–dC). Competitors used were oligonucleotides containing Site 1 (lanes 2–4), ma (lanes 5–7), Site 2 (lanes 8–10) and mb (lanes 11–13).

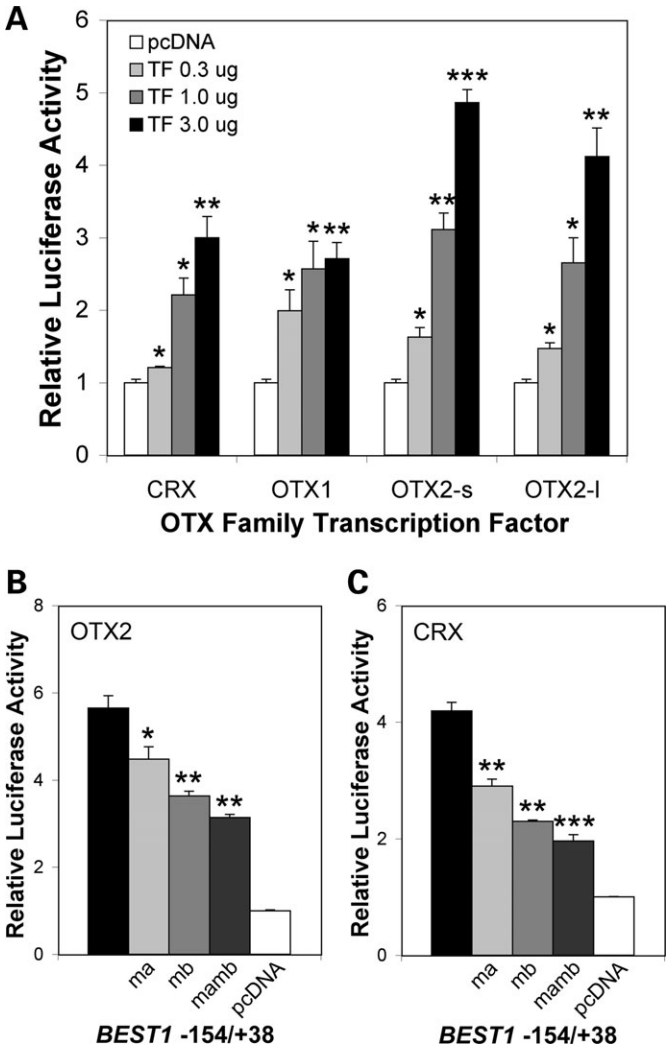

Figure 3. OTX factors modulate *BEST1* promoter activity through proximal binding sites. (**A**) OTX factors transactivate the *BEST1* promoter. A luciferase construct containing the *BEST1* −154 to +38 bp fragment was co-transfected into D407 cells with 0, 0.3, 1.0 or 3.0 μg of expression vector for CRX, OTX1, OTX2-s or OTX2-l and pRL-TK as internal control for normalization. The amount of expression plasmid was adjusted to a total 3.0 μg for each transfection by adding empty pcDNA3.1 vector. Relative luciferase activities (fold increase) were calculated as the ratio of the normalized luciferase activity with OTX factors to that with empty pcDNA3.1 (labeled as pcDNA and defined as 1). Transfection experiments were performed three times independently in duplicate each time. The values represent the mean and SD (bar). Results were statistically analyzed for each amount of expression vector compared with empty pcDNA3.1. Statistical significance is presented by $^{*}P < 0.05$, $^{**}P < 0.01$ and $^{***}P < 0.001$ throughout this figure. (**B**) Effect of OTX site mutation on OTX2 transactivation. Luciferase constructs containing wild-type sequence and mutation ma, mb or mamb in the *BEST1* −154 to +38 bp fragments were transfected into D407 cells together with an OTX2-s expression vector or empty pcDNA3.1 and pRL-TK as internal control for normalization. Relative luciferase activities (fold increase) were calculated as the ratio of the normalized luciferase activity with OTX2-s to that with empty pcDNA3.1 (defined as 1) for each luciferase construct. Transfection experiments were performed three times independently in duplicate each time. The values represent the mean and SEM (bar). Statistical significance was examined for each mutated construct compared with the wild-type construct. (**C**) Effect of OTX site mutation on CRX transactivation. Experimental design was the same as that described in (B) except that a CRX expression vector was used.

effects of the same mutated constructs introduced into mouse RPE cells by *in vivo* electroporation (Fig. 1D), consistent with the possibility that OTX2 and/or CRX-mediated transactivation might be responsible for the results observed *in vivo*.

Since it has been reported that OTX2 and MITF cooperatively activate some pigment-related gene promoters (11), and we previously showed that the *BEST1* promoter is regulated by MITF (42), we tested whether OTX2 and MITF also cooperatively activate the *BEST1* promoter. Co-transfection assays were carried out with *BEST1* promoter/luciferase constructs and expression vectors for both

OTX2 and MITF-M in D407 cells; however, no synergistic effect of these factors was observed on the *BEST1* promoter (data not shown).

Retinal pigment epithelium expresses both *OTX2* and *CRX* mRNA

To explore *in vivo* expression patterns, since obviously expression is necessary for biological activity, we used reverse transcription-polymerase chain reaction (RT-PCR) to analyze the expression of *CRX*, *OTX1* and *OTX2* mRNA in human RPE primary culture as well as RPE and retinal tissues. Rhodopsin (*RHO*), which is highly and specifically expressed in rod photoreceptors, was used as control to assess retinal contamination in the RPE RNA samples, and *BEST1* was used as an RPE marker. *OTX2* was highly expressed in both RPE and retina, whereas *OTX1* message was not detected in either tissue, consistent with reported expression patterns for both factors in adult eyes (5,7,23,60–63). In both RPE and retina, the predominant isoform of *OTX2* was *OTX2-s* (data not shown). *CRX* was expressed in the retina, but to our surprise it was also detected in the RPE, which has not been previously reported (Fig. 4A). This unexpected *CRX* expression in the RPE did not seem to be due to retinal contamination of the RPE samples, because *RHO* message was neither detected in either the RPE primary culture or RPE tissue, nor to false annealing of PCR primers to other OTX family members, since the *CRX* primers did not produce detectable bands with expression plasmids for either *OTX1* or *OTX2* as template.

We employed quantitative real-time PCR (qPCR) to quantify the relative expression levels of *CRX* in human RPE and retina using *GAPDH* as a control for normalization and *RHO* as a retinal marker for evaluating the degree of retinal contamination of RPE samples. The ratio of the *CRX* mRNA level in the RPE to that in the retina was substantially higher than the ratio of the *RHO* message level detected in the RPE to that in the retina, suggesting that the *CRX* mRNA detected in the RPE cannot simply be explained by retinal contamination of RPE samples (Fig. 4B). To check this finding in another species, we analyzed the relative expression levels of *CRX* and *RHO* in bovine RPE and retina by qPCR and found that the level of *CRX* expression in the RPE was even closer to that in the retina (Fig. 4C).

CRX genomic region has an open chromatin configuration in bovine retinal pigment epithelium

Since the detection of *CRX* message in the RPE did not appear to be simply due to contamination with retina RNA, we tried to obtain additional evidence that *CRX* was indeed transcribed in the RPE. We chose a DNase I hypersensitive site (DNase I HS) assay to analyze the genomic region around the transcription start site (TSS) of *CRX* in bovine RPE cells because the open nucleosomal structure observed around the TSS of actively transcribed genes is generally associated with increased DNase I sensitivity (64). For comparison, the TSS regions of two genes that are highly expressed in the RPE, *RPE65* and *BEST1*, and two genes that are not expressed in the RPE, *RHO* and albumin (*ALB*), were also analyzed as positive and negative controls, respectively. Since the TSS for the bovine orthologs of these genes was not known, we designed our studies based on the known TSSs of the human versions of the genes. Using a PCR-based assay (65,66), we confirmed that the assigned TSS regions of bovine *CRX*, *RHO* and *ALB* were hypersensitive to DNase I in retina, retina and liver where they were highly expressed, respectively (data not shown), and that those of bovine *RPE65* and *BEST1* showed hypersensitivity to DNase I in the RPE (see below). Bovine RPE nuclei were treated with a gradient of DNase I concentrations, the amount of undigested genomic DNA at the TSS region was quantified by qPCR, and the relative amount of undigested DNA in each sample was calculated as the ratio to the amount of intact genomic DNA in the control sample without DNase I (0 units, presented as 1). As expected, the region around the TSS of *RPE65* and *BEST1* was digested with low concentrations of DNase I, whereas that of *RHO* and *ALB* required much higher concentrations of DNase I to achieve similar levels of digestion (Fig. 4D and E). The sensitivity of the *CRX* TSS region to DNase I was between those of these two groups of genes, but closer to that for *RPE65* and *BEST1* (Fig. 4D). We also confirmed that these tentative TSS regions were not sensitive to DNase I digestion in tissues where the genes were not expressed. Among RPE, retina and liver, the region around the TSS of *CRX* was more resistant to DNase I in liver, as was that of *RHO* in RPE and liver, *ALB* in RPE and retina, *RPE65* in retina and liver and *BEST1* in retina and liver (data not shown). These results indicate that in the RPE the region around the TSS of *CRX* has a similar open nucleosomal structure to that of *RPE65* and *BEST1*, providing indirect evidence consistent with the expression data suggesting that *CRX* is actively transcribed in the RPE.

Bovine retinal pigment epithelium expresses CRX protein

We used Western blotting combined with immunoprecipitation (IP) of bovine RPE extracts to confirm the presence of CRX at the protein level. We used this combination of IP and Western blot analysis because of issues related to the sensitivity and specificity of available antibodies. We initially tried direct Western analysis with whole cell extracts of bovine RPE, retina and liver using the polyclonal anti-CRX antibody p261. Consistent with p261's reported specificity for CRX (67,68), we found using *in vitro* transcribed and translated proteins that the antibody reacted with CRX but not with OTX1 or OTX2 proteins (data not shown). However, in Westerns with the whole cell tissue extracts, although we did detect a signal of the predicted size in the RPE and retinal extracts, we also observed multiple non-specific bands in the negative control liver lane (data not shown). Similar testing of another anti-CRX antibody, monoclonal 4G11, gave almost opposite results where it did not react with the liver extract but with the *in vitro* transcribed and translated proteins it cross-reacted with both OTX1 and OTX2 (data not shown). In order to take advantage of the complementary specificities of the two antibodies, we developed a method that combined IP by p261 (which does not react with OTX1 and OTX2) with Western analysis using

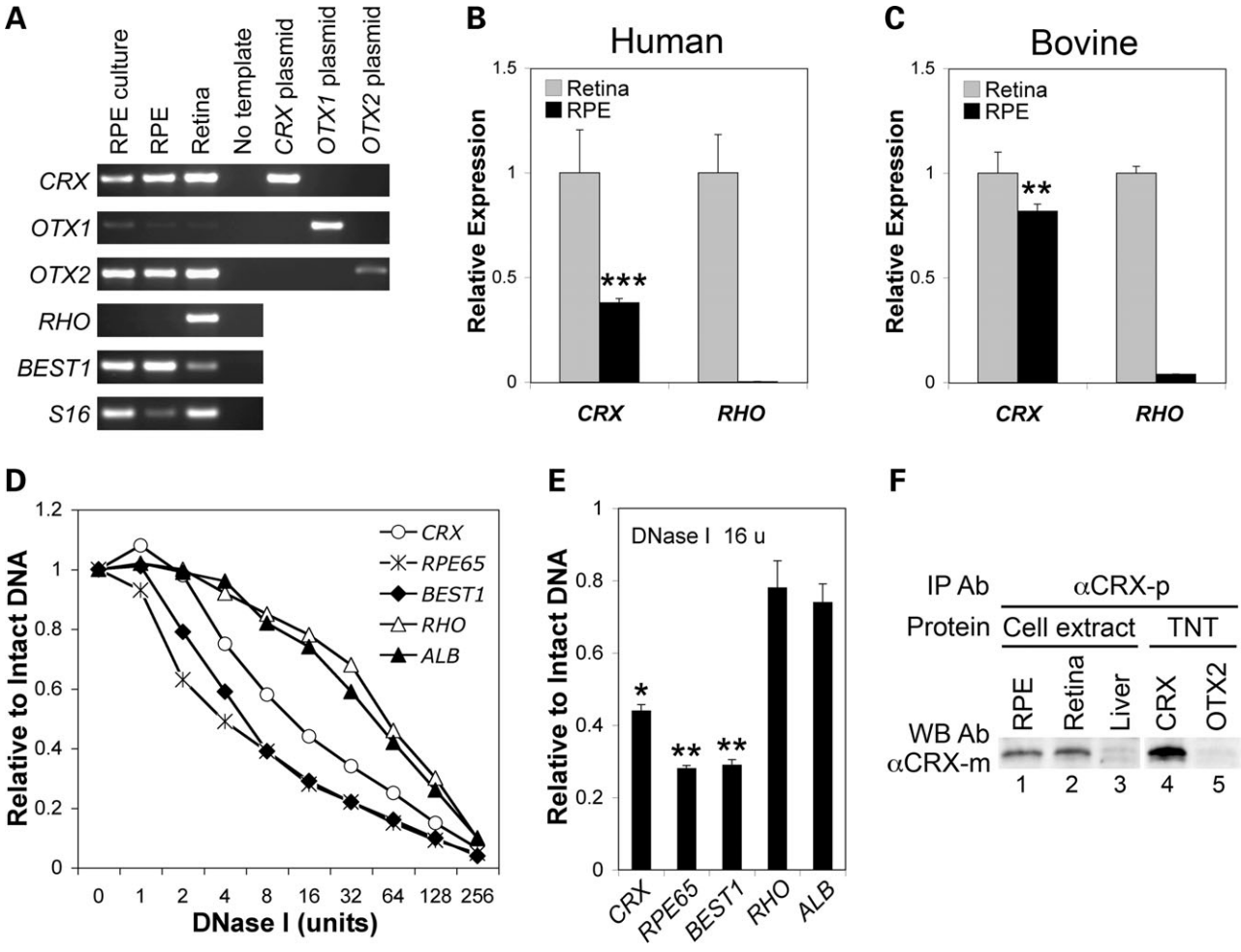

Figure 4. Retinal pigment epithelium expresses both *OTX2* and *CRX*. (**A**) Expression of *OTX* gene mRNA in human RPE and retina. The expression of *CRX*, *OTX1* and *OTX2* in human RPE primary culture and tissues of human RPE and retina was analyzed by reverse transcription-polymerase chain reaction along with control genes – *RHO* for retina, *BEST1* for RPE and *S16* for RNA quality and quantity. To confirm the specificity of PCR primers, plasmids containing each *OTX* cDNA were also included as template. (**B**) *CRX* expression in human RPE. The expression levels of *CRX*, *RHO* and control *GAPDH* were analyzed by reverse transcription-quantitative polymerase chain reaction (qPCR) in triplicates using pooled RPE and retinal RNAs prepared from human donor eyes. Based on threshold cycle (Ct) values, the expression level of *CRX* and *RHO* was normalized by that of *GAPDH*, and relative expression was calculated as the ratio of the normalized expression level in the RPE to that in the retina (defined as 1). The values represent the mean and SD (bar) of triplicate qPCR measurements. Difference in the relative expression in the RPE between *CRX* and *RHO* was statistically significant ($^{***}P < 0.001$). (**C**) *CRX* expression in bovine RPE. RPE and retinal RNAs were extracted from bovine eyes kept on ice for 48 h, and the expression levels of *CRX*, *RHO* and control *GAPDH* were analyzed in the same manner as in (B). Difference in the relative expression in the RPE between *CRX* and *RHO* was statistically significant ($^{**}P < 0.01$). (**D**) DNase I hypersensitive sites in RPE cells *in vivo*. RPE cell nuclei prepared from bovine eyes were digested with 0, 1, 2, 4, 8, 16, 32, 64, 128, 256 U of DNase I, and genomic DNAs of digested samples were purified and quantified. qPCR was performed using 30 ng genomic DNA of each sample with primers amplifying 200–250 bp fragments located around the TSS (−200 to +100 bp) of the indicated genes. Based on Ct values, the relative amount of PCR template in a sample was calculated as the ratio to the amount of PCR template in the undigested sample (intact DNA, defined as 1). The DNase I digestions were performed three times independently, and each sample was analyzed by qPCR in duplicate. The values represent the means. (**E**) Reproducibility of DNase I hypersensitive assay. The results with 16 U of DNase I shown in (D) are presented as the mean and SEM (bar) to demonstrate the reproducibility of the three biologically independent experiments. Differences were statistically analyzed for each gene compared with *RHO*, and statistical significance is shown by $^{*}P < 0.05$ and $^{**}P < 0.01$. (**F**) Expression of CRX protein in bovine RPE and retina. Based on the expectation that retina would contain the highest amount of CRX protein, 1000, 200 and 1000 μg of bovine RPE (lane 1), retina (lane 2) and liver (lane 3) whole cell extracts, respectively, were immunoprecipitated with anti-CRX polyclonal antibody p261 (labeled as αCRX-p). The immune-complexes were then collected with Protein A Sepharose, and bound proteins were eluted and analyzed by Western blotting with anti-CRX monoclonal antibody 4G11 (labeled as αCRX-m). As control to monitor the specificity of the IP–Western procedures, *in vitro* transcribed and translated CRX and OTX2 proteins (labeled as TNT; lanes 4 and 5, respectively) were also processed in parallel with the cell extracts.

4G11 (which does not react with liver proteins). A band of the expected size for CRX was detected in both the RPE and retinal extracts, but not in the negative control liver extracts (Fig. 4F). As control to monitor the specificity of the IP–Western procedure, we processed *in vitro* transcribed and translated CRX and OTX2 proteins (labeled as TNT) in parallel with the tissue extracts, and obtained a strong signal for CRX, but not for OTX2, indicating that the signal detected in the RPE and retinal extracts represented CRX. Based on the difference in the amount of protein input between the extracts (see figure legend), the results suggest that the level of CRX protein in bovine RPE is approximately 20% of that in bovine retina.

OTX2 and CRX bind to the *BEST1* proximal promoter *in vivo*

Chromatin immunoprecipitation (ChIP) was used with bovine RPE cells to assess whether OTX2 and CRX bind to the *BEST1* proximal promoter *in vivo*. We consistently obtained similar patterns for both OTX2 and CRX using the anti-OTX2 antibody ab21990 (Fig. 5A) and the anti-CRX antibody p261 (Fig. 5B), with the highest peak of relative enrichment at the −100 bp region and lower or no enrichment at the upstream and downstream regions in the RPE. In contrast, ChIP with bovine retina, in which both OTX2 and CRX are expressed but not *BEST1*, showed a relatively high background throughout the *BEST1* genomic locus without any peak of enrichement. ChIP with bovine liver, in which neither transcription factor nor *BEST1* are expressed, yielded a low background without any peak of enrichment throughout the *BEST1* genomic locus. As a known positive control, we assayed *RHO* as a target for both OTX2 and CRX in the retina and obtained an expected peak of relative enrichment at the −100 bp region (data not shown). In terms of the properties of the antibodies used in the ChIP experiments, the high specificity of the anti-CRX antibody p261 for CRX has already been described. Similar analysis of the anti-OTX2 antibody ab21990 revealed that it cross-reacted with CRX (data not shown). Therefore, the peak obtained by ChIP with ab21990 likely reflects binding of both OTX2 and CRX, although the relative proportions are difficult to assess. These ChIP results suggest strong and localized *in vivo* binding of both OTX2 and CRX at the *BEST1* proximal promoter in the RPE, but not in either the retina or liver, consistent with both factors being part of the regulatory network that controls *BEST1* expression in the RPE.

DISCUSSION

We previously demonstrated that two possible OTX factor-binding sites are present in the *BEST1* proximal promoter that is sufficient to direct RPE-specific expression in the eye (42,43). Based on this finding, we hypothesized that OTX2 might be an important factor in the modulation of *BEST1* expression. This seemed reasonable based on OTX2's expression pattern in the RPE and the RPE phenotype of *Otx2* knockout mice, which is more profound than that seen with knockouts of other OTX family members (7,26). In exploring this hypothesis, we obtained both expected and surprising results as discussed below. To test the functional importance of the two OTX-binding sites *in vivo*, quantitative assays using *in vivo* electroporation to transfer plasmid DNA directly into mouse RPE proved informative (58,59). The relative values of normalized luciferase activity driven by the *BEST1* promoter constructs in mouse RPE were different from those in D407 and SK-MEL-5 cell lines, as were the effects of the Site 1 (ma) and Site 2 (mb) mutations. These observations nicely demonstrate that transient transfection assays can be sensitive to the cellular environment in which they are performed, and therefore need to be carefully interpreted. Possible differences in the expression of transcription factors and interacting proteins need to be considered (69,70). As one example of differential transcription factor expression, among the three OTX genes, only *OTX1* message was detectable by RT-PCR in D407 and SK-MEL-5 cells (unpublished data), in contrast to fresh RPE tissue, which expresses *OTX2* but not *OTX1*. The results in mouse RPE reveal that although Sites 1 and 2 both seem to contribute to *BEST1* promoter activity *in vivo*, surprisingly the non-consensus Site 2 is functionally more important than the more canonical Site 1.

Given that members of the MITF–TFE family are important in *BEST1* expression (42), the results described indicate *BEST1* to be the first example of a non-pigment-related gene that is regulated by both MITF and OTX2 in the RPE. As intrinsic transcription factors mediating the effect of extrinsic signaling molecules on RPE development, MITF and OTX2 are essential for RPE specification and differentiation (3,4,6,7,10). Although a growing number of MITF direct targets other than pigment-related genes have been identified in melanocytes, mast cells and osteoclasts (6,10,71), the MITF direct targets in the RPE that have been identified to date, such as *TYR*, *TYRP1*, *DCT* (also known as *TYRP2*), *QNR71* and *GPR143* (also known as *OA1*) (4,72), are all melanin or melanosome-related. The situation of OTX2 in the RPE is similar in some way to that of MITF. OTX2 is critical for multiple aspects of eye development, including photoreceptor cell fate determination (62), terminal differentiation of photoreceptors and bipolar cells (61), and specification and differentiation of the RPE (5,7). However, OTX2 direct targets in the RPE described so far are limited to melanin or melanosome-related genes, such as *QNR71*, *Tyr*, *TYRP1* and *DCT* (11,41). Considering the essential roles of MITF and OTX2 in RPE development, it is highly likely that these two transcription factors are key components of the RPE transcriptional regulatory network, playing important roles in controlling expression of both pigment-related and non-pigment-related genes.

MITF and OTX2 physically interact and cooperatively activate the *QNR71* and *Tyr* promoters, suggesting that these factors function at the same hierarchical level (11). With the *TYRP1* promoter, however, although both factors are individually active, cooperative activation was not observed (11). With the *BEST1* promoter, we also failed to observe evidence of synergistic activity. It is unclear why MITF and OTX2 function cooperatively on some promoters, but not on the others, even when both types of promoters are activated by these factors individually. Although one possible explanation could be that the distance and/or orientation of binding sites for these factors may dictate how they interact, or the existence of binding sites for other factors nearby may influence their interaction, further studies are needed to answer this question.

An unexpected result in our studies was the finding of significant *CRX* expression in human and bovine RPE. Based on the data presented, the finding neither seem to be owing to a PCR artifact nor contamination of our RPE samples with retinal tissue. We also confirmed the CRX expression in bovine RPE cells at the protein level. Consistent with true *CRX* transcription in the RPE, we presented data that the *CRX* gene in the RPE has an open configuration and that the *BEST1* promoter is bound by both OTX2 and CRX *in vivo*. Although this finding seems surprising since it has not been

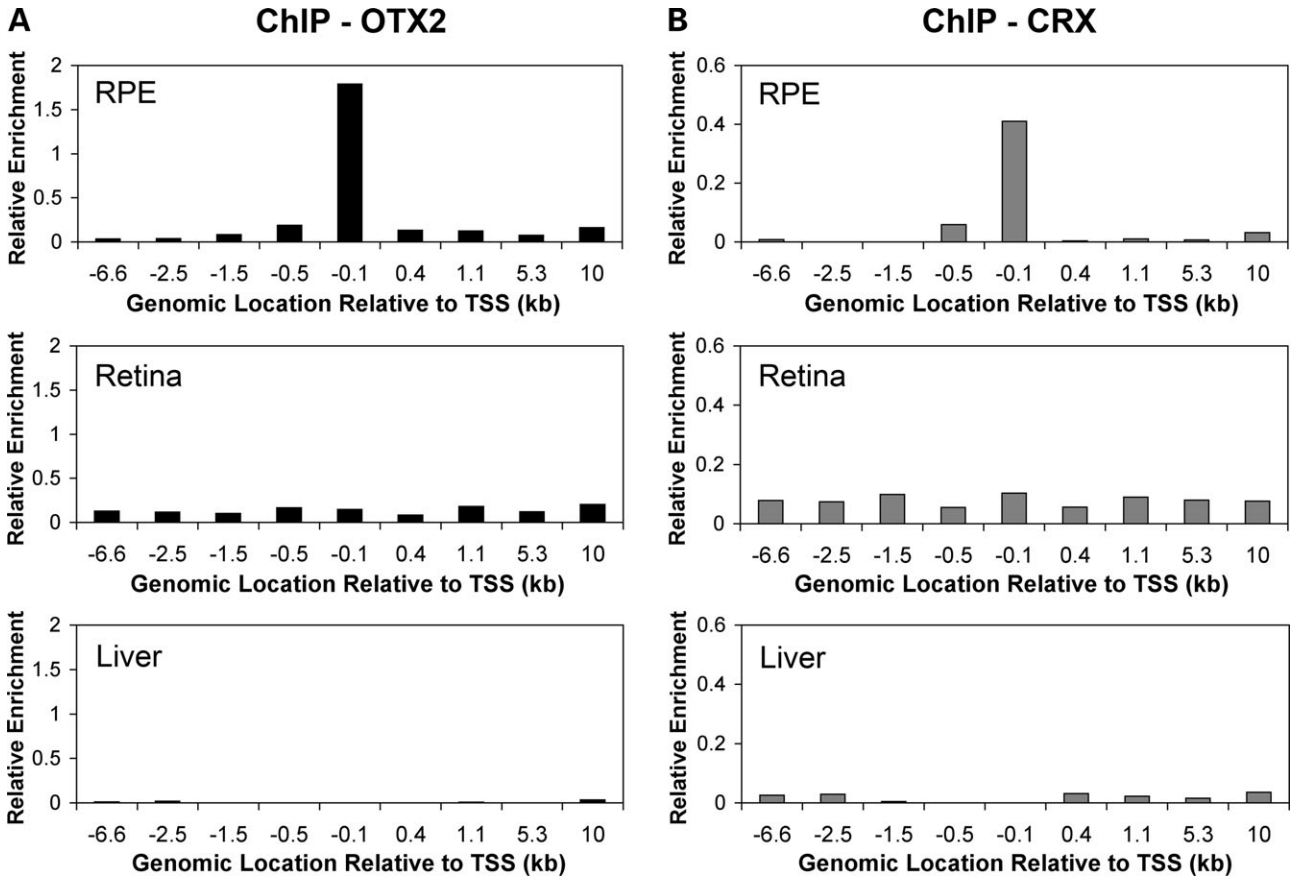

Figure 5. OTX2 and CRX bind to the *BEST1* proximal promoter *in vivo*. (**A**) Chromatin immunoprecipitation (ChIP) for OTX2. ChIP was performed using bovine RPE, retina and liver with anti-OTX2 antibody ab21990, and the final chromatin precipitates as well as diluted input DNA were analyzed by quantitative polymerase chain reaction (qPCR) in duplicate using primers amplifying 100–200 bp fragments in different regions of *BEST1* as indicated. Based on Ct values, relative enrichment of each genomic region was calculated as the ratio of the amount of PCR template in ChIP samples to that in the diluted input. Representative results are shown. The peak of relative enrichment was observed at the TSS region, with lower or no enrichment at the upstream and downstream regions, in the RPE but not in either the retina or liver. (**B**) ChIP for CRX. ChIP was performed and results are presented in the same manner as described in (A), except that anti-CRX antibody p261 was used. The relative enrichment patterns at these genomic locations were very similar to those observed with the anti-OTX2 antibody shown in (A).

previously reported, from an evolutionary point of view it may not be so surprising because *Otx5*, an ortholog of mammalian *Crx*, is expressed in the RPE of fish, frog and chick (28). Furthermore, since *Crx* itself is a direct target of OTX2 in retinal photoreceptors (62), and the expression of OTX2 in the RPE is well-established (4,5,7,28,60), it is reasonable that *CRX* may also be induced by OTX2 in the RPE. Supporting the possible biological significance of co-expression of CRX and MITF *in vivo*, it has been reported that transfected CRX can also cooperate with MITF to increase pigment granule expression in cultured quail neural retina cells, that CRX and MITF can act synergistically in the transactivation of the *QNR71* promoter, and that they can physically interact as measured by a pull-down assay (28).

Although we showed by ChIP that both OTX2 and CRX bind to the *BEST1* proximal promoter in bovine RPE cells, the extent to which CRX contributes to modulate *BEST1* expression *in vivo* is unclear. At least no obvious morphological change in the RPE was reported in *Crx* knockout mice (30), although *Crx* expression in mouse RPE has not been confirmed, and not much attention has been paid to the RPE related to *Crx* so far. This situation may in some ways be analogous to that of CRX and OTX2 in the retina. In retinal photoreceptor cells, while CRX has been known for a decade to be an essential transcription factor for terminal differentiation of both rod and cone cells (24,25,30,32), the importance of OTX2 was initially unrecognized. Later, using mice with conditional *Otx2* knockout as well as double knockouts for both *Otx2* and *Crx*, the important role of *Otx2* at both early and late stages of photoreceptor development was discovered (61,62). Other examples of redundant functions shared by members of the same transcription factor family are the functions of MITF–TFE family members. *Tfe3*'s role in osteoclast development is functionally redundant with that of *Mitf* and was revealed only after obtaining *Tfe3* null mice in an *Mitf* mutant background (73). We also demonstrated that MITF, TFE3 and TFEB can all transactivate the *BEST1* promoter, but the transactivating activity of TFE3 and TFEB was revealed only after using siRNA to significantly reduce the effects of MITF (42). The situation for OTX factors in the RPE may be similar. While the essential roles of OTX2 in RPE development are well-documented, discovering

CRX's possible role in the RPE will require future work. If *Crx* expression is confirmed in mouse RPE as well, mice with conditional *Crx* knockout targeted to the RPE as well as double knockouts for both *Otx2* and *Crx* will be invaluable tools.

In summary, we demonstrated that *BEST1* is a direct target of OTX2, and possibly CRX, in bovine RPE cells, and showed for the first time that *CRX* is expressed in human and bovine RPE. These results provide the first example of a non-pigment-related gene that is regulated by both MITF and OTX2, two transcription factors essential for RPE development and differentiation, expanding our understanding of the processes regulating development of the RPE.

MATERIALS AND METHODS

Plasmid construction

A *BEST1* promoter/*lacZ* reporter construct was made for transgenic mouse studies using the PCR-generated fragment from −104 to +38 bp relative to the TSS (upstream −; downstream +) as previously described (43).

BEST1 promoter/luciferase reporter constructs containing the fragments −154 to +38 and −104 to +38 bp in pGL2-Basic vector, which contains firefly luciferase gene (Promega, Madison, WI, USA), were generated previously (43). Two new *BEST1* promoter/luciferase reporter constructs in pGL2-Basic vector were made using the promoter fragments −136 to +38 and −120 to +38 bp generated by PCR with primers listed in Supplementary Material, Table S1, as previously described (43).

Mutated *BEST1* promoter/luciferase constructs in the context of the −154 to +38 bp fragment were made using PCR with synthetic long oligonucleotides containing mutation in Site 1 (−127 to −122 bp, AGATTA to AG*CGGC*, designated ma), mutation in Site 2 (−81 to −76 bp, GGCTTA to GGC*GGC*, mb) and both (mamb) (Supplementary Material, Table S1). All fragments were blunt-ligated into SmaI site of pGL2-Basic vector and verified by sequencing.

Expression vectors containing bovine *CRX* cDNA in pcDNA3.1/His C vector (Invitrogen, Carlsbad, CA, USA) and human *MITF-M* cDNA in pcDNA3.1/Myc-His(−) B vector (Invitrogen) were made previously (24,43). To construct expression vectors for human OTX1, OTX2-s (short isoform) and OTX2-l (long isoform), cDNAs were generated by RT-PCR using 1 μg total RNA extracted from human RPE primary culture as template and primer pairs containing restriction sites, EcoRI site in forward primers and BamHI site in reverse primers (Supplementary Material, Table S1). The short and long isoforms of *OTX2* cDNAs were obtained from natural splice variants. The cDNA fragments were inserted into EcoRI/BamHI sites downstream of the cytomegalovirus (CMV) promoter in pcDNA3.1/Myc-His(−) B vector.

Generation and analysis of transgenic mice

Transgenic mice carrying a construct containing the *BEST1* −104 to +38 bp fragment fused to a *lacZ* reporter (*BEST1* promoter/*lacZ*) were generated and analyzed as previously described (43).

Cell culture

D407 human RPE cell line was maintained as reported (74). SK-MEL-5 human melanoma cell line (75) was cultured in the medium recommended by the American Type Culture Collection (ATCC, Manassas, VA, USA).

Transient transfection

Transient transfection assays were performed as previously described (42,43), except that dual luciferase assays were used in this study. Plasmid DNA for each 60 mm dish included 3 μg of a firefly luciferase construct and 0.1 ng of pRL-CMV containing *Renilla* luciferase gene (Promega) as an internal control for transfection efficiency. Because we found that OTX1 and OTX2 activate the CMV promoter in control pRL-CMV, we instead utilized pRL-TK containing *Renilla* luciferase gene driven by the thymidine kinase (TK) promoter (Promega) as control for co-transfection studies with expression vectors. However, OTX1 activates the TK promoter as well; therefore, we used double normalization, first by *Renilla* luciferase activity and then by comparing the normalized values with that of empty pGL2-Basic vector. For these co-transfection studies, DNA mixture for each dish included 3 μg of a firefly luciferase construct, 0, 0.3, 1.0, or 3.0 μg of an expression vector, and 1 ng of pRL-TK, and the total amount of expression vector was adjusted to 3.0 μg by adding empty pcDNA3.1 vector when necessary. Transfections were performed three independent times in duplicate each time, and cell lysates were analyzed using Dual-Luciferase Reporter System (Promega). Firefly luciferase activities were normalized by *Renilla* luciferase activities, and relative luciferase activities were calculated as the ratio of the normalized luciferase activity with constructs containing *BEST1* promoter fragments to that with empty pGL2-Basic vector. To assess the effects of OTX factors on the *BEST1* promoter, relative luciferase activities (fold increase) were calculated as the ratio of the normalized luciferase activity with OTX expression vectors to that with empty pcDNA3.1 vector. To evaluate the effects of OTX site mutations on the transactivation by OTX factors, relative luciferase activities were calculated as the ratio of the normalized luciferase activity with 3.0 μg OTX expression vectors to that with empty pcDNA3.1 for each *BEST1* promoter/luciferase construct.

In vivo electroporation

The development of an *in vivo* electroporation method and its application in the analysis of the *BEST1* promoter were described previously (42,58,59). Subretinal injection followed by *in vivo* electroporation into 6–8 week-old BALB/cJ mice was performed using 1 μl of phosphate-buffered saline (PBS) containing 0.5 μg of a *BEST1* promoter/luciferase construct and 0.25 ng of pRL-CMV as control to normalize transduction variability among eyes. Three days after electroporation, mice were euthanized, eyes were dissected to remove cornea and lens, and cell lysates of the posterior portion of the eye were prepared using 100 μl of Reporter Lysis Buffer (Promega) (58). Firefly and *Renilla* luciferase activities were measured using Dual-Luciferase Reporter System, and relative

luciferase activities were calculated as described above for cell transfection.

Electrophoretic mobility shift assay (EMSA)

Electrophoretic mobility shift assay was performed according to standard methods as previously described (43,76), except that proteins to be tested, CRX, OTX1, OTX2-s, OTX2-l and control luciferase, were generated by *in vitro* transcription and translation using the TnT T7 Quick Coupled Transcription–Translation System (Promega). The efficiency of protein synthesis was checked in a separate set of reactions by ^{35}S-methionine-labeling. Two annealed oligonucleotide probes, one corresponding to −135 to −112 bp that contains Site 1 and the other corresponding to −91 to −68 bp that contains Site 2, were generated together with probes containing mutation of Site 1 (AGATTA to AG*CGGC*, ma) and Site 2 (GGCTTA to GGC*GGC*, mb). Labeled probe was incubated with 3 μl of *in vitro* transcribed and translated proteins in binding solution (10 mM Tris–Cl, pH 7.9, 100 mM KCl, 5 mM $MgCl_2$, 1 mM ethylene diamine tetraacetic acid (EDTA), 1 mM dithiothreitol, 0.5 mM phenylmethylsulfonyl fluoride, 5% glycerol) containing 1 μg of poly (dI–dC) on ice for 30 min and analyzed. X-ray films were exposed without intensifying screens overnight (∼15 h) to avoid saturation of signals as well as to maximize the linearity of the signal intensity. For cold oligomer competition experiments, ^{32}P-labeled Site 1 and 2 probes were first mixed with 10-, 100- and 1000-fold molar excess of unlabeled annealed oligonucleotides corresponding to probes Site 1, ma, Site 2 and mb, then added to binding solutions containing 1 μl OTX2-s protein.

RT-PCR and quantitative real-time PCR (qPCR)

Total RNAs were extracted from RPE primary culture as well as RPE and retinal tissues prepared from human donor eyes using TRIzol reagent (Invitrogen). The expression of OTX family genes was analyzed by RT-PCR along with control genes, *RHO* for retina, *BEST1* for RPE and *S16* for RNA quality and quantity. First-strand cDNA was synthesized from 1 μg of total RNA with an oligo(dT) primer using SuperScript III reverse transcriptase (Invitrogen), and PCR was performed (Supplementary Material, Table S1). To confirm that PCR products are gene-specific among the three OTX genes, 1 pg of expression plasmids containing each human OTX gene cDNA were also used as template for PCR reaction. To discriminate between human *OTX2* transcript variants 1 (isoform a, long) and 2 (isoform b, short), a pair of primers was used to amplify 113 and 89 bp fragments for long and short variants, respectively (Supplementary Material, Table S1).

To rule out the possibility that the detection of *CRX* transcript in the RPE was due to the contamination of retinal RNA into RPE RNA samples, the message level of *CRX* and *RHO* was measured by qPCR in both human and bovine eye tissues. For human samples, retina and RPE RNAs were analyzed with the same primer pairs as described above and control *GAPDH* primers (Supplementary Material, Table S1). For bovine samples, eyes obtained from a local slaughterhouse were kept on ice for different lengths of time (1, 24, 48 and 72 h), then dissected equatorially, the retina was collected by peeling, RPE cells were collected by gentle scraping and total RNAs were extracted using TRIzol reagent (Invitrogen). In a pilot set of studies we found that incubation for 48 h maintained RNA quality and minimized retinal contamination of the RPE, as measured by the presence of *RHO* mRNA—at 1 h there was still strong attachment between the retina and RPE, and at 72 h the retina was very fragile. Therefore, we used RNA samples prepared at 48 h for experiments. After the first-strand cDNA was synthesized as described above, qPCR was performed with the primers listed in Supplementary Material, Table S1. qPCR was performed using iQ SYBR Green Supermix (Bio-Rad, Hercules, CA, USA) with iQ5 Real-Time PCR Detection System (Bio-Rad). Based on crossing point (threshold cycle, Ct) values, the expression level of each gene was normalized by that of *GAPDH*, and relative expression was calculated as the ratio of the normalized expression level in the RPE to that in the retina (defined as 1).

DNase I hypersensitive site (DNase I HS) assay

RPE cell nuclei from 20 bovine eyes were treated according to a published protocol (77), modified as follows: RPE cells collected by gentle scraping were washed in PBS containing 5 mM EDTA, dispersed in 10 ml of the same buffer by several strokes of Dounce homogenization with a B pestle, passed through two layers of cheesecloth and centrifuged at $1000 \times g$ for 5 min. The pellets were resuspended in 7 ml of buffer A containing 0.5% Nonidet P-40, homogenized by 30 strokes with a B pestle, kept on ice for 10 min, homogenized again by additional 10 strokes and centrifuged at $1000 \times g$ for 5 min. The pellets (nuclei) were resuspended in 10 ml of buffer A containing 0.5% Nonidet P-40, aliquoted into 10 microcentrifuge tubes, washed with 1 ml of buffer A, resuspended in 100 μl of buffer A for each tube and digested by adding 100 μl of DNase I buffer containing various amounts of DNase I (0, 1, 2, 4, 8, 16, 32, 64, 128 or 256 U; Roche, Indianapolis, IN, USA) and incubating at 25°C for 10 min. Digestion was stopped by adding 200 μl of stop buffer, and samples were treated with 50 μg/ml proteinase K at 55°C overnight. Genomic DNAs were purified by gentle phenol–chloroform extraction and ethanol precipitation, resuspended in 10 mM Tris–HCl pH 8.0, quantified by UV spectrophotometry, and DNA concentrations were adjusted to 10 ng/μl. qPCR was performed using 3 μl of each sample (30 ng genomic DNA) with the primers that were designed to amplify 200–250 bp fragments located between −200 and +100 bp relative to the TSS for *CRX*, *RPE65*, *BEST1*, *RHO* and *ALB* (Supplementary Material, Table S1) (65,66). Based on Ct values, the relative amount of PCR template in a sample was calculated as the ratio to the amount of PCR template in the undigested sample (intact DNA, presented as 1). The DNase I digestion experiments were performed three times independently, and each sample was analyzed by qPCR in duplicate.

Immunoprecipitation and Western blotting

First, we compared the efficiency of protein extraction from bovine RPE by Western blot analysis with anti-OTX2

antibody ab21990 (rabbit polyclonal, Abcam, Cambridge, UK) because OTX2 expression in the RPE is well known. Surprisingly, we found that whole cell extracts generated by a freeze-thaw (FT) lysis method showed a stronger signal than either whole cell extracts or even nuclear extracts prepared by a detergent-based lysis method that is more commonly used. Therefore, we decided to use the FT whole cell extracts for our IP–Western blot analyses.

The whole cell extracts of bovine RPE, retina and liver were made by four cycles of the FT lysis method consisting of freezing in liquid nitrogen and thawing on ice in FT lysis buffer [600 mM KCl, 20 mM Tris–Cl (pH 7.8), 20% glycerol, protease inhibitor cocktail (Sigma)]. The extracts of bovine RPE (1000 μg), retina (200 μg) and liver (1000 μg) were diluted into a total of 300 μl of IP lysis buffer [150 mM NaCl, 50 mM Tris–Cl (pH 8.0), 1% IGEPAL CA-630, protease inhibitor cocktail], centrifuged at 12 000 × *g* for 10 min at 4°C to remove insoluble particles, and mixed with 50 μl of Protein A Sepharose (GE Healthcare, Piscataway, NJ, USA) at 4°C for 1 h with gentle agitation for pre-clearing. After centrifugation at 12 000 × *g* for 30 s at 4°C, the supernatants were transferred to new microcentrifuge tubes, incubated with 1 μg of anti-CRX antibody p261 (rabbit polyclonal, a kind gift from Dr. Shiming Chen, Washington University, St Louis, MO, USA) (67) at 4°C for 2 h with gentle agitation, and the protein–antibody complexes were collected with 50 μl of Protein A Sepharose at 4°C for 3 h with gentle mixing. After centrifugation at 12 000 × *g* for 30 s at 4°C, Sepharose beads with the precipitated protein–antibody complexes were washed five times, twice with 1 ml of IP lysis buffer, twice with 1 ml of IP lysis buffer containing 450 mM NaCl instead of 150 mM NaCl and once with 1 ml of wash buffer [50 mM Tris–Cl (pH 8.0)], and bound proteins were eluted in 30 μl of sample buffer [125 mM Tris–Cl (pH 6.8), 2% SDS, 10% glycerol, 5% (v/v) β-mercaptoethanol]. After heating at 70°C for 10 min, 15 μl of each eluted sample were resolved by SDS–PAGE and transferred to Hybond-P polyvinylidene fluoride membrane (GE Healthcare). The membrane was blocked in Tris-buffered saline containing Tween-20 (TBST) [10 mM Tris–Cl (pH 7.5), 100 mM NaCl, 0.1% Tween-20] containing 5% non-fat dry milk at room temperature for 1 h and probed with anti-CRX antibody 4G11 (H00001406-M02, mouse monoclonal, Abnova, Taiwan) at 1:2000 dilution in TBST containing 5% non-fat dry milk at 4°C overnight with gentle agitation. After washing with TBST for 10 min four times, the membrane was incubated with horseradish peroxidase-conjugated anti-mouse IgG antibody (GE Healthcare) at 1:10 000 dilution at room temperature for 1 h with gentle agitation, and protein signals were visualized using ECL Plus Western blotting detection reagents and ECL Hyperfilm (GE Healthcare). As control to monitor the specificity and efficiency of the IP–Western procedures, 10 μl of CRX or OTX2 protein generated by *in vitro* transcription and translation as described earlier for EMSA were also processed in the same manner in parallel with the FT whole cell extracts.

Chromatin immunoprecipitation (ChIP)

ChIP was performed using bovine RPE, retina and liver as previously described (42,78) with the following modifications. For ChIP with RPE cells, bovine eyes obtained from a local slaughterhouse were dissected to remove cornea, lens and retina, and RPE/choroid eye cups were directly cross-linked in 1% formaldehyde in PBS at room temperature for 15 min. Cross-linking was stopped by adding glycine at a final concentration 0.125 M and incubating at room temperature for 5 min, eye cups were washed twice in PBS, and RPE cells were collected by gentle scraping. Once RPE cell suspension was obtained, the rest of ChIP procedures were performed as previously described. ChIP with retina and liver tissues was performed in the same manner as previously described (42,78). The anti-OTX2 antibody ab21990 and the anti-CRX antibody p261 were used to precipitate chromatin–protein complexes. The final DNA precipitates were resuspended in 120 μl of TE (10 mM Tris–HCl pH 8.0, 1 mM EDTA), and 3 μl of each sample and diluted input (1:50) were used for qPCR in duplicate with the primers designed to amplify 100–200 bp fragments in different regions of *BEST1* (Supplementary Material, Table S1). Based on Ct values, the relative enrichment of each genomic region was calculated as the ratio of the amount of each PCR template in ChIP samples to that in diluted input.

Statistical analysis

Unpaired *t*-test was used for statistical analysis.

ACKNOWLEDGEMENTS

We thank Shiming Chen for providing the anti-CRX antibody p261. This study was supported in part by unrestricted funds from Research to Prevent Blindness, Inc. and generous gifts from Robert and Clarice Smith and the Guerrieri Family Foundation. P.A.C. is the George S. and Dolores Dore Eccles Professor of Ophthalmology and Neuroscience; D.J.Z. is the Guerrieri Professor of Genetic Engineering and Molecular Ophthalmology at the Wilmer Eye Institute and is a recipient of a Research to Prevent Blindness Senior Investigator Award.

Conflict of Interest statement. None declared.

FUNDING

National Institutes of Health (EY015410 to N.E., EY016398 to N.E. and EY001765 to Wilmer Eye Institute.).

REFERENCES

1. Bok, D. (1993) The retinal pigment epithelium: a versatile partner in vision. *J. Cell Sci. Suppl.*, **17**, 189–195.
2. Thumann, G. and Hinton, D.R. (2001) Cell biology of the retinal pigment epithelium. In Ryan, S.J. (ed.), *Retina*, 3rd edn. Mosby, St. Louis, USA, Vol. 3, pp. 104–121.
3. Bharti, K., Nguyen, M.T., Skuntz, S., Bertuzzi, S. and Arnheiter, H. (2006) The other pigment cell: specification and development of the pigmented epithelium of the vertebrate eye. *Pigment Cell Res.*, **19**, 380–394.
4. Martinez-Morales, J.R., Rodrigo, I. and Bovolenta, P. (2004) Eye development: a view from the retina pigmented epithelium. *Bioessays*, **26**, 766–777.

5. Bovolenta, P., Mallamaci, A., Briata, P., Corte, G. and Boncinelli, E. (1997) Implication of OTX2 in pigment epithelium determination and neural retina differentiation. *J. Neurosci.*, **17**, 4243–4252.
6. Goding, C.R. (2000) Mitf from neural crest to melanoma: signal transduction and transcription in the melanocyte lineage. *Genes Dev.*, **14**, 1712–1728.
7. Martinez-Morales, J.R., Signore, M., Acampora, D., Simeone, A. and Bovolenta, P. (2001) Otx genes are required for tissue specification in the developing eye. *Development*, **128**, 2019–2030.
8. Nakayama, A., Nguyen, M.T., Chen, C.C., Opdecamp, K., Hodgkinson, C.A. and Arnheiter, H. (1998) Mutations in microphthalmia, the mouse homolog of the human deafness gene MITF, affect neuroepithelial and neural crest-derived melanocytes differently. *Mech. Dev.*, **70**, 155–166.
9. Nguyen, M. and Arnheiter, H. (2000) Signaling and transcriptional regulation in early mammalian eye development: a link between FGF and MITF. *Development*, **127**, 3581–3591.
10. Steingrimsson, E., Copeland, N.G. and Jenkins, N.A. (2004) Melanocytes and the microphthalmia transcription factor network. *Annu. Rev. Genet.*, **38**, 365–411.
11. Martinez-Morales, J.R., Dolez, V., Rodrigo, I., Zaccarini, R., Leconte, L., Bovolenta, P. and Saule, S. (2003) OTX2 activates the molecular network underlying retina pigment epithelium differentiation. *J. Biol. Chem.*, **278**, 21721–21731.
12. Hemesath, T.J., Steingrimsson, E., McGill, G., Hansen, M.J., Vaught, J., Hodgkinson, C.A., Arnheiter, H., Copeland, N.G., Jenkins, N.A. and Fisher, D.E. (1994) Microphthalmia, a critical factor in melanocyte development, defines a discrete transcription factor family. *Genes Dev.*, **8**, 2770–2780.
13. Hodgkinson, C.A., Moore, K.J., Nakayama, A., Steingrimsson, E., Copeland, N.G., Jenkins, N.A. and Arnheiter, H. (1993) Mutations at the mouse microphthalmia locus are associated with defects in a gene encoding a novel basic-helix-loop-helix-zipper protein. *Cell*, **74**, 395–404.
14. Hughes, M.J., Lingrel, J.B., Krakowsky, J.M. and Anderson, K.P. (1993) A helix-loop-helix transcription factor-like gene is located at the mi locus. *J. Biol. Chem.*, **268**, 20687–20690.
15. Tassabehji, M., Newton, V.E. and Read, A.P. (1994) Waardenburg syndrome type 2 caused by mutations in the human microphthalmia (MITF) gene (see comments). *Nat. Genet.*, **8**, 251–255.
16. Tietz, W. (1963) A syndrome of deaf-mutism associated with albinism showing dominant autosomal inheritance. *Am. J. Hum. Genet.*, **15**, 259–264.
17. Bumsted, K.M. and Barnstable, C.J. (2000) Dorsal retinal pigment epithelium differentiates as neural retina in the microphthalmia (mi/mi) mouse. *Invest. Ophthalmol. Vis. Sci.*, **41**, 903–908.
18. Hertwig, P. (1942) Neue Mutationen und Kopplungsgruppen bei der Hausmaus. *Z. Indukt. Abstammungs-Vererbungsl.*, **80**, 220–246.
19. Packer, S.O. (1967) The eye and skeletal effects of two mutant alleles at the microphthalmia locus of Mus musculus. *J. Exp. Zool.*, **165**, 21–46.
20. Acampora, D., Annino, A., Tuorto, F., Puelles, E., Lucchesi, W., Papalia, A. and Simeone, A. (2005) Otx genes in the evolution of the vertebrate brain. *Brain Res. Bull.*, **66**, 410–420.
21. Finkelstein, R., Smouse, D., Capaci, T.M., Spradling, A.C. and Perrimon, N. (1990) The orthodenticle gene encodes a novel homeo domain protein involved in the development of the Drosophila nervous system and ocellar visual structures. *Genes Dev.*, **4**, 1516–1527.
22. Simeone, A. (1998) Otx1 and Otx2 in the development and evolution of the mammalian brain. *EMBO J.*, **17**, 6790–6798.
23. Simeone, A., Acampora, D., Mallamaci, A., Stornaiuolo, A., D'Apice, M.R., Nigro, V. and Boncinelli, E. (1993) A vertebrate gene related to orthodenticle contains a homeodomain of the bicoid class and demarcates anterior neuroectoderm in the gastrulating mouse embryo. *EMBO J.*, **12**, 2735–2747.
24. Chen, S., Wang, Q.L., Nie, Z., Sun, H., Lennon, G., Copeland, N.G., Gilbert, D.J., Jenkins, N.A. and Zack, D.J. (1997) Crx, a novel Otx-like paired-homeodomain protein, binds to and transactivates photoreceptor cell-specific genes. *Neuron*, **19**, 1017–1030.
25. Furukawa, T., Morrow, E.M. and Cepko, C.L. (1997) Crx, a novel otx-like homeobox gene, shows photoreceptor-specific expression and regulates photoreceptor differentiation. *Cell*, **91**, 531–541.
26. Matsuo, I., Kuratani, S., Kimura, C., Takeda, N. and Aizawa, S. (1995) Mouse Otx2 functions in the formation and patterning of rostral head. *Genes Dev.*, **9**, 2646–2658.
27. Simeone, A., Puelles, E. and Acampora, D. (2002) The Otx family. *Curr. Opin. Genet. Dev.*, **12**, 409–415.
28. Plouhinec, J.L., Leconte, L., Sauka-Spengler, T., Bovolenta, P., Mazan, S. and Saule, S. (2005) Comparative analysis of gnathostome Otx gene expression patterns in the developing eye: implications for the functional evolution of the multigene family. *Dev. Biol.*, **278**, 560–575.
29. Plouhinec, J.L., Sauka-Spengler, T., Germot, A., Le Mentec, C., Cabana, T., Harrison, G., Pieau, C., Sire, J.Y., Veron, G. and Mazan, S. (2003) The mammalian Crx genes are highly divergent representatives of the Otx5 gene family, a gnathostome orthology class of orthodenticle-related homeogenes involved in the differentiation of retinal photoreceptors and circadian entrainment. *Mol. Biol. Evol.*, **20**, 513–521.
30. Furukawa, T., Morrow, E.M., Li, T., Davis, F.C. and Cepko, C.L. (1999) Retinopathy and attenuated circadian entrainment in Crx-deficient mice. *Nat. Genet.*, **23**, 466–470.
31. Ragge, N.K., Brown, A.G., Poloschek, C.M., Lorenz, B., Henderson, R.A., Clarke, M.P., Russell-Eggitt, I., Fielder, A., Gerrelli, D., Martinez-Barbera, J.P. *et al.* (2005) Heterozygous mutations of OTX2 cause severe ocular malformations. *Am. J. Hum. Genet.*, **76**, 1008–1022.
32. Freund, C.L., Gregory-Evans, C.Y., Furukawa, T., Papaioannou, M., Looser, J., Ploder, L., Bellingham, J., Ng, D., Herbrick, J.A., Duncan, A. *et al.* (1997) Cone-rod dystrophy due to mutations in a novel photoreceptor-specific homeobox gene (CRX) essential for maintenance of the photoreceptor. *Cell*, **91**, 543–553.
33. Freund, C.L., Wang, Q.L., Chen, S., Muskat, B.L., Wiles, C.D., Sheffield, V.C., Jacobson, S.G., McInnes, R.R., Zack, D.J. and Stone, E.M. (1998) De novo mutations in the CRX homeobox gene associated with Leber congenital amaurosis. *Nat. Genet.*, **18**, 311–312.
34. Sohocki, M.M., Sullivan, L.S., Mintz-Hittner, H.A., Birch, D., Heckenlively, J.R., Freund, C.L., McInnes, R.R. and Daiger, S.P. (1998) A range of clinical phenotypes associated with mutations in CRX, a photoreceptor transcription-factor gene. *Am. J. Hum. Genet.*, **63**, 1307–1315.
35. Swain, P.K., Chen, S., Wang, Q.L., Affatigato, L.M., Coats, C.L., Brady, K.D., Fishman, G.A., Jacobson, S.G., Swaroop, A., Stone, E. *et al.* (1997) Mutations in the cone-rod homeobox gene are associated with the cone-rod dystrophy photoreceptor degeneration. *Neuron*, **19**, 1329–1336.
36. Acampora, D., Mazan, S., Lallemand, Y., Avantaggiato, V., Maury, M., Simeone, A. and Brulet, P. (1995) Forebrain and midbrain regions are deleted in Otx2−/− mutants due to a defective anterior neuroectoderm specification during gastrulation. *Development*, **121**, 3279–3290.
37. Ang, S.L., Jin, O., Rhinn, M., Daigle, N., Stevenson, L. and Rossant, J. (1996) A targeted mouse Otx2 mutation leads to severe defects in gastrulation and formation of axial mesoderm and to deletion of rostral brain. *Development*, **122**, 243–252.
38. Acampora, D., Mazan, S., Avantaggiato, V., Barone, P., Tuorto, F., Lallemand, Y., Brulet, P. and Simeone, A. (1996) Epilepsy and brain abnormalities in mice lacking the *Otx1* gene. *Nat. Genet.*, **14**, 218–222.
39. Acampora, D., Avantaggiato, V., Tuorto, F., Barone, P., Perera, M., Choo, D., Wu, D., Corte, G. and Simeone, A. (1999) Differential transcriptional control as the major molecular event in generating Otx1−/− and Otx2−/− divergent phenotypes. *Development*, **126**, 1417–1426.
40. Acampora, D., Avantaggiato, V., Tuorto, F., Briata, P., Corte, G. and Simeone, A. (1998) Visceral endoderm-restricted translation of Otx1 mediates recovery of Otx2 requirements for specification of anterior neural plate and normal gastrulation. *Development*, **125**, 5091–5104.
41. Takeda, K., Yokoyama, S., Yasumoto, K., Saito, H., Udono, T., Takahashi, K. and Shibahara, S. (2003) OTX2 regulates expression of DOPAchrome tautomerase in human retinal pigment epithelium. *Biochem. Biophys. Res. Commun.*, **300**, 908–914.
42. Esumi, N., Kachi, S., Campochiaro, P.A. and Zack, D.J. (2007) VMD2 promoter requires two proximal E-box sites for its activity in vivo and is regulated by the MITF-TFE family. *J. Biol. Chem.*, **282**, 1838–1850.
43. Esumi, N., Oshima, Y., Li, Y., Campochiaro, P.A. and Zack, D.J. (2004) Analysis of the VMD2 promoter and implication of E-box binding factors in its regulation. *J. Biol. Chem.*, **279**, 19064–19073.
44. Petrukhin, K., Koisti, M.J., Bakall, B., Li, W., Xie, G., Marknell, T., Sandgren, O., Forsman, K., Holmgren, G., Andreasson, S. *et al.* (1998) Identification of the gene responsible for Best macular dystrophy. *Nat. Genet.*, **19**, 241–247.
45. Duta, V., Szkotak, A.J., Nahirney, D. and Duszyk, M. (2004) The role of bestrophin in airway epithelial ion transport. *FEBS Lett.*, **577**, 551–554.

46. Marquardt, A., Stohr, H., Passmore, L.A., Kramer, F., Rivera, A. and Weber, B.H. (1998) Mutations in a novel gene, VMD2, encoding a protein of unknown properties cause juvenile-onset vitelliform macular dystrophy (Best's disease). *Hum. Mol. Genet.*, **7**, 1517–1525.
47. Sun, H., Tsunenari, T., Yau, K.W. and Nathans, J. (2002) The vitelliform macular dystrophy protein defines a new family of chloride channels. *Proc. Natl. Acad. Sci. USA*, **99**, 4008–4013.
48. Tsunenari, T., Sun, H., Williams, J., Cahill, H., Smallwood, P., Yau, K.W. and Nathans, J. (2003) Structure-function analysis of the bestrophin family of anion channels. *J. Biol. Chem.*, **278**, 41114–41125.
49. Hartzell, H.C., Qu, Z., Yu, K., Xiao, Q. and Chien, L.T. (2008) Molecular physiology of bestrophins: multifunctional membrane proteins linked to best disease and other retinopathies. *Physiol. Rev.*, **88**, 639–672.
50. Wimmers, S., Karl, M.O. and Strauss, O. (2007) Ion channels in the RPE. *Prog. Retin. Eye Res.*, **26**, 263–301.
51. Marmorstein, L.Y., Wu, J., McLaughlin, P., Yocom, J., Karl, M.O., Neussert, R., Wimmers, S., Stanton, J.B., Gregg, R.G., Strauss, O. *et al.* (2006) The light peak of the electroretinogram is dependent on voltage-gated calcium channels and antagonized by bestrophin (best-1). *J. Gen. Physiol.*, **127**, 577–589.
52. Rosenthal, R., Bakall, B., Kinnick, T., Peachey, N., Wimmers, S., Wadelius, C., Marmorstein, A. and Strauss, O. (2006) Expression of bestrophin-1, the product of the VMD2 gene, modulates voltage-dependent Ca2+ channels in retinal pigment epithelial cells. *FASEB J.*, **20**, 178–180.
53. Yu, K., Xiao, Q., Cui, G., Lee, A. and Hartzell, H.C. (2008) The best disease-linked Cl- channel hBest1 regulates Ca V 1 (L-type) Ca2+ channels via src-homology-binding domains. *J. Neurosci.*, **28**, 5660–5670.
54. Allikmets, R., Seddon, J.M., Bernstein, P.S., Hutchinson, A., Atkinson, A., Sharma, S., Gerrard, B., Li, W., Metzker, M.L., Wadelius, C. *et al.* (1999) Evaluation of the Best disease gene in patients with age-related macular degeneration and other maculopathies. *Hum. Genet.*, **104**, 449–453.
55. Seddon, J.M., Afshari, M.A., Sharma, S., Bernstein, P.S., Chong, S., Hutchinson, A., Petrukhin, K. and Allikmets, R. (2001) Assessment of mutations in the Best macular dystrophy (VMD2) gene in patients with adult-onset foveomacular vitelliform dystrophy, age-related maculopathy, and bull's-eye maculopathy. *Ophthalmology*, **108**, 2060–2067.
56. Yardley, J., Leroy, B.P., Hart-Holden, N., Lafaut, B.A., Loeys, B., Messiaen, L.M., Perveen, R., Reddy, M.A., Bhattacharya, S.S., Traboulsi, E. *et al.* (2004) Mutations of VMD2 splicing regulators cause nanophthalmos and autosomal dominant vitreoretinochoroidopathy (ADVIRC). *Invest. Ophthalmol. Vis. Sci.*, **45**, 3683–3689.
57. Burgess, R., Millar, I.D., Leroy, B.P., Urquhart, J.E., Fearon, I.M., De Baere, E., Brown, P.D., Robson, A.G., Wright, G.A., Kestelyn, P. *et al.* (2008) Biallelic mutation of BEST1 causes a distinct retinopathy in humans. *Am. J. Hum. Genet.*, **82**, 19–31.
58. Kachi, S., Esumi, N., Zack, D.J. and Campochiaro, P.A. (2006) Sustained expression after nonviral ocular gene transfer using mammalian promoters. *Gene Ther.*, **13**, 798–804.
59. Kachi, S., Oshima, Y., Esumi, N., Kachi, M., Rogers, B., Zack, D.J. and Campochiaro, P.A. (2005) Nonviral ocular gene transfer. *Gene Ther.*, **12**, 843–851.
60. Baas, D., Bumsted, K.M., Martinez, J.A., Vaccarino, F.M., Wikler, K.C. and Barnstable, C.J. (2000) The subcellular localization of Otx2 is cell-type specific and developmentally regulated in the mouse retina. *Brain Res. Mol. Brain Res.*, **78**, 26–37.
61. Koike, C., Nishida, A., Ueno, S., Saito, H., Sanuki, R., Sato, S., Furukawa, A., Aizawa, S., Matsuo, I., Suzuki, N. *et al.* (2007) Functional roles of Otx2 transcription factor in postnatal mouse retinal development. *Mol. Cell. Biol.*, **27**, 8318–8329.
62. Nishida, A., Furukawa, A., Koike, C., Tano, Y., Aizawa, S., Matsuo, I. and Furukawa, T. (2003) Otx2 homeobox gene controls retinal photoreceptor cell fate and pineal gland development. *Nat. Neurosci.*, **6**, 1255–1263.
63. Rath, M.F., Morin, F., Shi, Q., Klein, D.C. and Moller, M. (2007) Ontogenetic expression of the Otx2 and Crx homeobox genes in the retina of the rat. *Exp. Eye Res.*, **85**, 65–73.
64. Boeger, H., Griesenbeck, J., Strattan, J.S. and Kornberg, R.D. (2003) Nucleosomes unfold completely at a transcriptionally active promoter. *Mol. Cell*, **11**, 1587–1598.
65. Dorschner, M.O., Hawrylycz, M., Humbert, R., Wallace, J.C., Shafer, A., Kawamoto, J., Mack, J., Hall, R., Goldy, J., Sabo, P.J. *et al.* (2004) High-throughput localization of functional elements by quantitative chromatin profiling. *Nat. Methods*, **1**, 219–225.
66. McArthur, M., Gerum, S. and Stamatoyannopoulos, G. (2001) Quantification of DNaseI-sensitivity by real-time PCR: quantitative analysis of DNaseI-hypersensitivity of the mouse beta-globin LCR. *J. Mol. Biol.*, **313**, 27–34.
67. La Spada, A.R., Fu, Y.H., Sopher, B.L., Libby, R.T., Wang, X., Li, L.Y., Einum, D.D., Huang, J., Possin, D.E., Smith, A.C. *et al.* (2001) Polyglutamine-expanded ataxin-7 antagonizes CRX function and induces cone-rod dystrophy in a mouse model of SCA7. *Neuron*, **31**, 913–927.
68. Peng, G.H. and Chen, S. (2005) Chromatin immunoprecipitation identifies photoreceptor transcription factor targets in mouse models of retinal degeneration: new findings and challenges. *Vis. Neurosci.*, **22**, 575–586.
69. Alge, C.S., Suppmann, S., Priglinger, S.G., Neubauer, A.S., May, C.A., Hauck, S., Welge-Lussen, U., Ueffing, M. and Kampik, A. (2003) Comparative proteome analysis of native differentiated and cultured dedifferentiated human RPE cells. *Invest. Ophthalmol. Vis. Sci.*, **44**, 3629–3641.
70. Cai, H. and Del Priore, L.V. (2006) Gene expression profile of cultured adult compared to immortalized human RPE. *Mol. Vis.*, **12**, 1–14.
71. Hershey, C.L. and Fisher, D.E. (2004) Mitf and Tfe3: members of a b-HLH-ZIP transcription factor family essential for osteoclast development and function. *Bone*, **34**, 689–696.
72. Vetrini, F., Auricchio, A., Du, J., Angeletti, B., Fisher, D.E., Ballabio, A. and Marigo, V. (2004) The microphthalmia transcription factor (Mitf) controls expression of the ocular albinism type 1 gene: link between melanin synthesis and melanosome biogenesis. *Mol. Cell. Biol.*, **24**, 6550–6559.
73. Steingrimsson, E., Tessarollo, L., Pathak, B., Hou, L., Arnheiter, H., Copeland, N.G. and Jenkins, N.A. (2002) Mitf and Tfe3, two members of the Mitf-Tfe family of bHLH-Zip transcription factors, have important but functionally redundant roles in osteoclast development. *Proc. Natl. Acad. Sci. USA*, **99**, 4477–4482.
74. Davis, A.A., Bernstein, P.S., Bok, D., Turner, J., Nachtigal, M. and Hunt, R.C. (1995) A human retinal pigment epithelial cell line that retains epithelial characteristics after prolonged culture. *Invest. Ophthalmol. Vis. Sci.*, **36**, 955–964.
75. Carey, T.E., Takahashi, T., Resnick, L.A., Oettgen, H.F. and Old, L.J. (1976) Cell surface antigens of human malignant melanoma: mixed hemadsorption assays for humoral immunity to cultured autologous melanoma cells. *Proc. Natl. Acad. Sci. USA*, **73**, 3278–3282.
76. Nie, Z., Chen, S., Kumar, R. and Zack, D.J. (1996) RER, an evolutionarily conserved sequence upstream of the rhodopsin gene, has enhancer activity. *J. Biol. Chem.*, **271**, 2667–2675.
77. Reitman, M., Lee, E., Westphal, H. and Felsenfeld, G. (1993) An enhancer/locus control region is not sufficient to open chromatin. *Mol. Cell. Biol.*, **13**, 3990–3998.
78. Qian, J., Esumi, N., Chen, Y., Wang, Q., Chowers, I. and Zack, D.J. (2005) Identification of regulatory targets of tissue-specific transcription factors: application to retina-specific gene regulation. *Nucleic Acids Res.*, **33**, 3479–3491.